# Determining the impact of facet roughness on etched facet InP laser devices operating at telecom wavelengths, making comparisons to theoretical models.

Tristan T. Burman[1], Jash Patel[2], Huma Ashraf[2], Tarran Grange[2], Samuel Shutts[1], Peter M. Smowton[1]

[1]School of Physics and Astronomy, Cardiff University, CF24 3AA, UK,
[2]KLA Corporation (SPTS Division), Ringland Way, Newport, NP18 2TA, UK
Email: BurmanT@cardiff.ac.uk; SmowtonPM@cardiff.ac.uk

**Keywords: Optoelectronic Integration, InP Lasers, Etched Facets**

**Abstract**

**This work independently determines the roughness and reflectivity of InP etched facet broad area lasers operating at 1550nm and compares the results to those predicted. The etched facet devices were found to have an RMS roughness of (24±7)nm and reflectivity (56±43)% of that of a cleaved facet. This differs slightly with the predicted value from the D. A. Stocker model of (70±14)%. The roughness profile of the etched facet differs from the assumed Gaussian distribution of the model, suggesting that other surface features beyond the RMS roughness considered by the model may have an impact on reflectivity.**

## INTRODUCTION

Optoelectronic devices are advancing in a manner remarkably similar to that of electronics over the last fifty years, with devices being miniaturized and integrated circuits being developed with an increasing number of integrated optoelectronic functions on chip. The laser is considered one of the more difficult components to integrate, and further research is necessary to produce efficient full wafer manufacturing processes that can be applied over large substrates for dense integration of lasers and other components. Traditionally laser facets are produced by cleaving, but as this involves breaking the wafer into pieces it is inappropriate for monolithic integrated circuits, and wet etching methods are unable to reliably produce the vertical profiles required. Dry etching can achieve vertical profiles using methods preferred in large scale manufacture. However, dry etching does tend to introduce an increased roughness of the facet and other vertical (or sidewall) surfaces, and the process must be optimized to reduce this.

The impact the facet roughness has on the laser device performance is yet to be fully understood. There is a seemingly commonly-used belief that an RMS roughness below that of the emission wavelength divided by an arbitrary value will produce a "tolerable" or X percent loss in efficiency [1]; the exact values tend to vary across different materials, emission wavelengths and institutions. Models do exist that attempt to better relate the RMS roughness of a surface to reflectivity and therefore laser performance [2]. The models are most often used when attempting to deduce the facet reflectivity of a device from a measured roughness or vice versa. However, these models are often developed for a single material and are rarely verified on real world devices.

Material systems such as GaN have a crystal structure that is not ideal for creating the parallel smooth facets required by lasers via cleaving methods [3]. As such, research into manufacturing GaN etched facets is well established [4]. The recent push for optoelectronic integration using monolithic integration, has led to a need, in materials that can easily form cleaved facet lasers such as InP, to utilize etched facet designs [5]. InP is however one of the more difficult materials to dry etch, due to the poor volatility of the etch products. While it is true that facets with low reflectivity can still be made to lase by increasing the cavity length and therefore the round-trip gain, a low reflectivity can impact other aspects of device performance such as threshold current.

This work measures both the facet roughness and device performance of InP based laser devices operating at telecom wavelengths manufactured on 100mm wafers.

## DEVICE FABRICATION

The InP laser device structure used in this work is comprised of six compressively strained InGaAsP quantum well's within InP cladding designed to emit at 1550nm. Aluminum containing structures were avoided to prevent any effects which may occur from oxidation of the aluminum at the facet. The lasers are manufactured as broad area laser devices using a single dry etch step. A broad area laser structure was selected as opposed to those more commonly seen in typical telecoms applications as the manufacturing process is much easier and the wide ridge will minimize any negative impact the sidewall roughness has on device performance. This should result in data that is dependent on facet roughness alone.

The devices have been designed in such a way that both cleaved faced and etched facets can be produced from the same wafer. Each cleaved facet device on the wafer is paired with an identical copy that uses an etched facet, this is shown pre cleave in Fig. 1. This arrangement allows for direct comparisons between the two facet types and minimizes any variation due to material or manufacturing uniformity.

The laser cavities are 200µm wide with cavity lengths varying between 100µm - 1000µm. A 700nm thick $SiO_2$ hardmask was used for the dry etch and was patterned using direct write lithography. Initial dry etch optimizations were conducted on InP substrate wafers before transferring the recipe to the broad area device mask on InP epi-structure material. The single InP deep dry etch was performed on a SPTS ICP etch tool using a chlorine-based chemistry. Finally coplanar contacts were deposited. To minimize any damage to the laser facets that may occur from removing the insulating $SiO_2$ hardmask layers, the facet is first protected with a photoresist while a small section of the hardmask is removed. The p-contact is then deposited into this hole making contact with the upper most layer of the device structure.

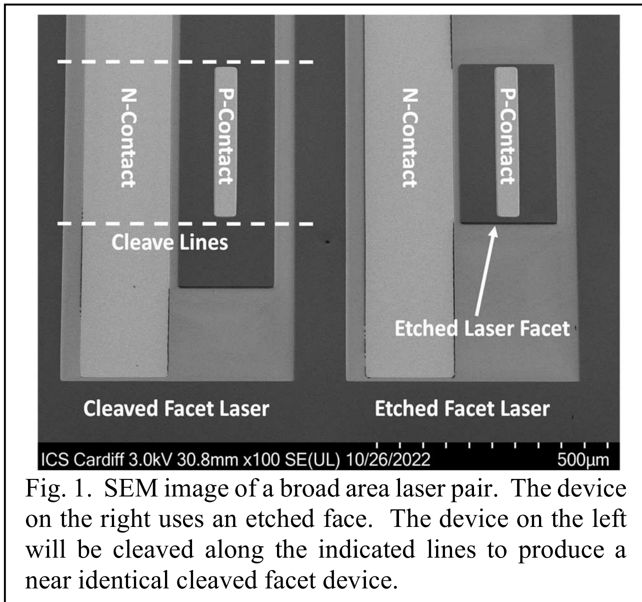

Fig. 1. SEM image of a broad area laser pair. The device on the right uses an etched face. The device on the left will be cleaved along the indicated lines to produce a near identical cleaved facet device.

METHODOLOGY

Optical power versus current (PI) and current-voltage (IV) measurements were taken of all etched facet devices across the wafer using a semi-automatic wafer mapper system with an integrating sphere, where the light emitted from the device at large angle is collected by the detector. This means while the threshold current can be determined accurately the measured slope efficiency is below the true value. Once the etched facet results were complete, sample tiles from the wafer center and edge were cleaved from the wafer for further measurement. The sidewall roughness of the etched facets was measured using a Bruker Dimension Icon AFM using the peak force tapping ScanAsyst imaging mode. To achieve this the samples are mounted at an inclination, which paired with the angle of the AFM probe allows for measurements the full height of the facets to be taken. This was repeated at multiple points across the sample tiles to determine the facet roughness.

Once all etched facet device data was collected, the sample tiles are lapped, reducing the tile thickness in order to produce a higher quality cleaved facet. Each tile was lapped to approximately 140µm as a compromise between fragility, the onset of wafer bow and ease of cleaving. It is often suggested that the shortest cavity lengths you can cleave from a sample and maintain a high-quality facet is approximately two and a half times the sample thickness. Therefore, cleaved facet devices with cavity lengths below approximately 350µm will likely be of a lower quality. In addition to this the material thickness prevented any cleaved facet devices with a cavity length below 250µm to be manufactured successfully. After cleaving the devices, the facets are inspected, and any displaying cleave damage are discarded. Finally, the devices are mounted and undergo PI and IV measurements.

From the PI measurements, the threshold current for each device can be determined using the second derivative threshold calculation. Considering the p-contact dimensions allows for the threshold current density to be calculated and plotted against the inverse cavity length. The gradient of the resulting linear relation is proportional to the facet reflectivity. Assuming cleaved facet devices have a reflectivity near that of a perfectly smooth surface allows the relative reflectivity of the etched devices to be determined.

RESULTS AND DISCUSSION

Fig. 2. shows an AFM image of one of the etched facet devices. A sizable portion of the roughness seen in this figure can be attributed to a defect that resembles draped curtains, this type of defect is often linked back to the mask patterning process. This work used direct write lithography which can produce aliasing defects within the mask which is then transferred to the material during the etch. As a result of this defect, the manufacture process has been updated and contact lithography will be used in future work to minimize facet roughness. The RMS roughness of the etched facet devices around the region of the epi-structure was found to be (24±7)nm. Using the commonly used D. A. Stocker model [2] this facet roughness is predicted to produce a reflectivity of (70±14)% that of a perfectly smooth surface.

Etched facet devices below 250µm failed to achieve a lasing action, likely due to the increased facet roughness. Improving the manufacture process to reduce facet roughness could allow the shorter cavity lengths to lase. The minimum cavity length for cleaved facets is determined by the material thickness which is limited due to the material fragility and stress. The lapped InP tiles were so fragile that many cleaved facet devices were lost due to breakages while cleaving and handling, with many facets being of a low quality, especially for cavity lengths below 350µm. As a result of these issues, there were only a small number of cleaved facet devices that achieved lasing action. The device mask has since been restructured to make the cleaving and handling easier, along with altering the cleaving process to minimize device losses and improve facet quality. This will improve yield and quality of the cleaved facet devices in future works.

Fig. 3. Shows a plot of threshold current density against the inverse cavity length for both the etched and cleaved facet

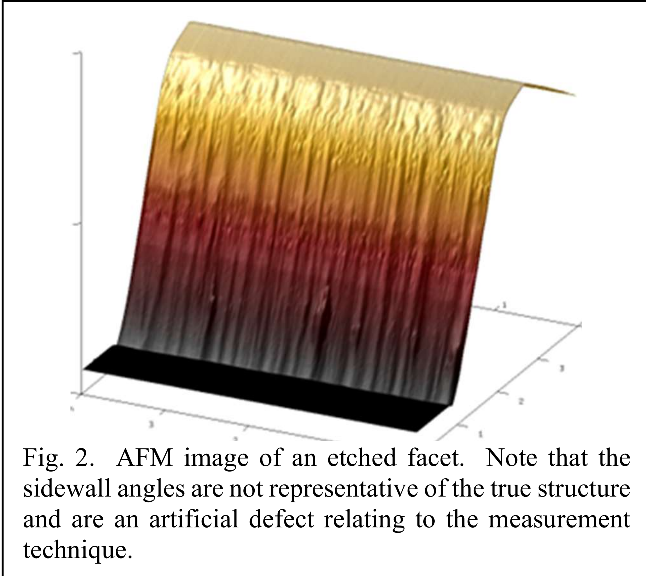

Fig. 2. AFM image of an etched facet. Note that the sidewall angles are not representative of the true structure and are an artificial defect relating to the measurement technique.

devices. Here it can be clearly seen that the cleaved facet devices return lower threshold current densities along with a shallower gradient. Using $m = K \ln\left(\frac{1}{R^2}\right)$, where $m$ is the gradient, $K$ is a constant and $R$ is the average power reflectivity of the facets, and assuming the cleaved facet has a perfectly smooth InP-air facet with a reflectivity of $R = 0.262$, the constant $K$ can be determined. This same relation can now be used to determine the average power reflectivity of the etched facet devices. This returns a reflectivity of (0.15±0.11) or (56±43)% that of the cleaved devices. The large standard deviation on this result is partly due to the small number of cleaved facet devices for this comparison returning a large standard deviation in the gradient. The previously mentioned processing improvements will improve yield for both etched and cleaved facet devices reducing gradient errors and increasing precision.

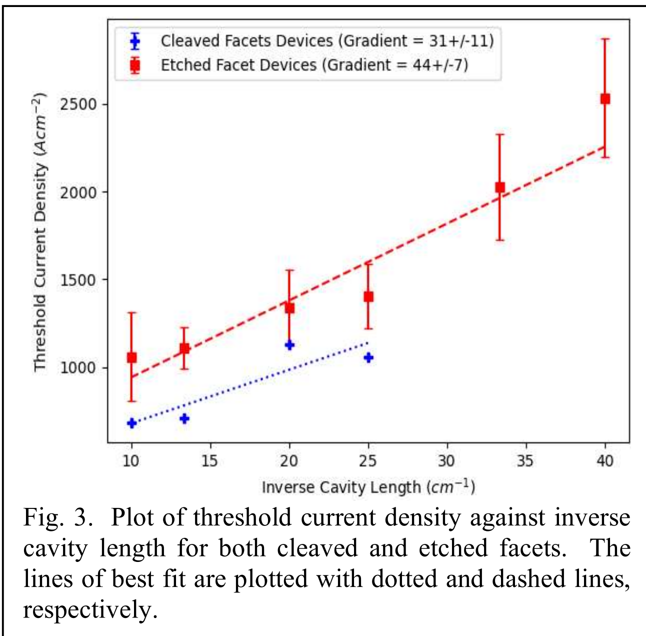


Fig. 3. Plot of threshold current density against inverse cavity length for both cleaved and etched facets. The lines of best fit are plotted with dotted and dashed lines, respectively.

The AFM measurements do not only provide RMS roughness data but can provide a range of additional surface texture parameters. One interesting point to note, is that the D. A. Stocker model assumes the facet roughness follows a Gaussian distribution. Using AFM techniques, the surface kurtosis (Sku) of the facet can be calculated. A Gaussian distribution would return a Sku=3, the etched facets return Sku=(5.3±2.2). Demonstrating that the facet roughness is more concentrated around the zero-displacement point and the distribution is more spike like. Additionally, the skewness (Ssk) determines the bias of the roughness distribution. The etched facets returned a Ssk=(1.1±0.6), showing that the distribution is skewed below the mean plane. These AFM measurements portray a roughness distribution that is quite different than the Gaussian distribution assumed by the model.

Compiling the AFM measurements of all etched facets into a histogram allows for the overall roughness distribution to be determined. The roughness distribution shown in Fig. 4. matches what was suggested by the Sku and Ssk measurements, a spiked distribution that is skewed below the mean plane. The measured roughness profile of the etched facet devices differs from the Gaussian distribution assumed by the model. The exact cause for this distribution is not yet fully understood, nor is it known if this distribution is typical of an etched facet. However, it is clear that the distribution assumed by the model is failing to account for a large portion of the roughness below the mean plane and overestimating roughness above for these facets, potentially offering an explanation of the discrepancy between the models and experimental results. This also suggests that there could be other surface features that could have an impact on the roughness that is not being considered by the model. This could include surface uniformity, max peak/pit heights and/or peak density.

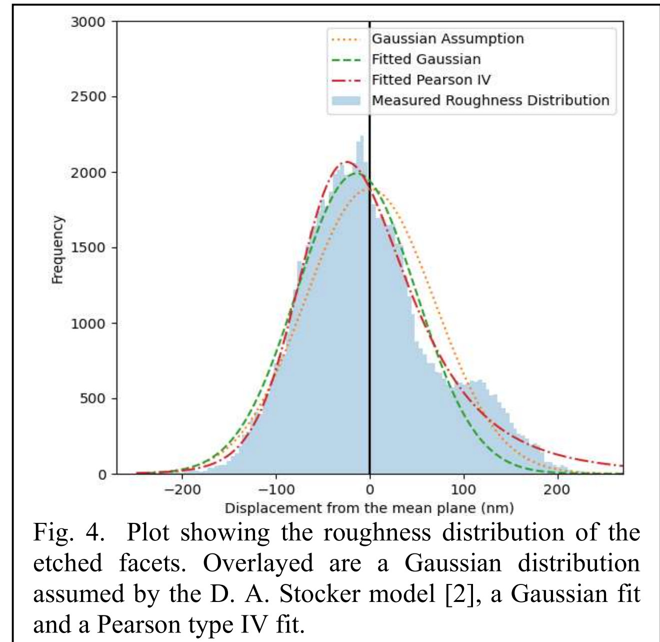


Fig. 4. Plot showing the roughness distribution of the etched facets. Overlayed are a Gaussian distribution assumed by the D. A. Stocker model [2], a Gaussian fit and a Pearson type IV fit.

Fitting a Gaussian distribution to the AFM roughness data shifts the center point below the plane, resulting in a closer fit. The improved fitted Gaussian distribution can then be used in the D. A. Stocker model which returns a reflectivity of 39.2% for this roughness distribution. This small change in roughness distribution has caused a significant shift in the predicted reflectivity. Further improving the roughness distribution fit could improve the model's accuracy. Pearsons type IV distribution accounts for parameters such as Sku and Ssk, additionally it simplifies to a Pearsons type VII distribution when Ssk=0 and can simplify further to a Gaussian distribution under certain conditions. This Pearsons type IV distribution seen in Fig. 4. provides an improved fit to the roughness distribution measured, which could lead to increased model accuracy. However, this distribution is known for being significantly more complex to implement into mathematical models. Metalog distributions are an alternative that are simpler to implement while allowing a wide degree of shape flexibility.

Despite the large standard deviation in the facet reflectivity results, these findings suggest that there may be aspects of facet roughness that are not being considered by the D. A. Stocker model causing potential discrepancies between the predicted and measured results.

## CONCLUSIONS

In conclusion, etched facet devices with an RMS roughness of (24±7)nm returns a facet reflectivity of (56±43)% that of a cleaved facet device, which is assumed to be perfectly smooth, along with an increased threshold current density. The D. A. Stocker model [2] predicts a facet with this roughness should produce a reflectivity of (70±14)%. The large standard deviation on the measured reflectivity is likely largely due to the low yield of cleaved facet devices, making a definitive statement on if the model agrees with experiment difficult. AFM measurements of the etched facet devices allowed for the roughness profile to be determined, the kurtosis was found to be (5.3±2.2) and the skewness (1.1±0.6), corresponding to a spiked distribution that skews below the surfaces mean plane. This profile differs from the mean plane centered Gaussian assumed by the model. Small adjustments to this distribution to better fit the measured roughness can lead to significant changes to the predicted result. This, along with other unaccounted surface parameters could be a cause of the large difference between experiment and prediction.

Several aspects of the advantages of etched facet devices have also been demonstrated. Wafer scale processing and characterization of devices allowed a sizable number of devices to be both manufactured and tested at wafer scale. This is something that would take a significant amount of time for cleaved facet devices, especially with more complex devices that require additional facet coating steps. Although the shortest length etched facet devices failed to achieve a lasing action, likely due to the higher facet roughness, it does demonstrate that shorter cavity length lasers than what can be realistically achieved using cleaved facets are possible with etched facets.

Multiple improvements to the device manufacturer process have been identified during this work and have been implemented for future iterations. These improvements along with additional process optimizations will help reduce facet roughness, increase cleaved facet yield and provide additional data points to identify the underlying relation between facet roughness, reflectivity and device performance.

## ACKNOWLEDGEMENTS

Device fabrication was conducted at the KLA Corp (SPTS Division) site in Newport, South Wales and in the cleanroom of the ERDF-funded Institute for Compound Semiconductors (ICS) at Cardiff University with assistance from both KLA and ICS staff. This work was supported by the Engineering and Physical Science Research Council EP/S024441/1 along with KLA.

## REFERENCES

[1] Francis, D. A., et al. *Effect of facet roughness on etched facet semiconductor laser diodes*. Applied Physics Letters 68, 1598–1600 (1996)

[2] D. A. Stocker, et al. *Facet roughness analysis for In-GaN/GaN lasers with cleaved facets,* Applied Physics Letters 73, 25–1927 (1998)

[3] A. Behfar, et al. *Etched facet technology for GaN and blue lasers. In Gallium Nitride Materials and Devices,* Proceedings of SPIE vol. 6121, 214-221 (2006)

[4] J. He, et al. *On-wafer fabrication of cavity mirrors for InGaN-based laser diode grown on Si,* Sci Rep 8, 7922 (2018)

[5] M. Nicolas, et al. *Fabrication process for low-cost GaInAsP/InP etched-facet photodetectors,* Proceedings of SPIE vol. 5731, (2005)

[6] Hildebrandt, L., et al. *Antireflection-coated blue GaN laser diodes in an external cavity and doppler-free indium absorption spectroscopy* Appl. Opt. 42, 2110-2118 (2003)

## ACRONYMS

RMS: Root Mean Square
GaN: Gallium Nitride
InP: Indium Phosphide
InGaAsP: Indium Gallium Arsenide Phosphide
SEM: Scanning Electron Microscopy
$SiO_2$: Silicon dioxide
AFM: Atomic Force Microscopy
Sku: Kurtosis
Ssk: Skewness